Modeling of Base Metal Dissolution Behavior during Transient Liquid-Phase Brazing

H. NAKAGAWA, C.H. LEE, and T.H. NORTH

Detailed finite difference modeling of dissolution during transient liquid-phase (TLP) brazing of nickel using Ni-11 wt pct P and Ni-14 wt pct Cr-10 wt pct P filler metals is carried out assuming *infinite* and *finite* heating rates between the filler melting temperature (T_m) and the brazing temperature (T_b). Two conditions are modeled during brazing, namely, where the liquid width due to base metal dissolution is *unrestrained* (variable) and where the liquid width is kept *constant* due to expulsion of excess liquid during the brazing process. The time required for completion of dissolution is proportional to the square of the filler metal thickness when an infinite heating rate between T_m and T_b is assumed. This occurs for both for constant and unrestrained liquid width situations. Also, the advance of the solid-liquid interface is approximately related to the reciprocal of the square root of the solute diffusivity in the liquid, except in the final stages of the dissolution process. When a multicomponent filler metal composition (Ni-14 wt pct Cr-10 wt pct P) is used, the time for completion of dissolution exceeds that when using a simple binary filler metal composition. The phosphorous concentration in the liquid approaches that of the liquidus line when the heating rate between T_m and T_b decreases and thin filler metals are used. This tendency can be estimated using a homogenizing index (z) which combines the effects of filler metal thickness, diffusivity in the liquid, brazing temperature and heating rate, and a distribution index (a). When thick filler metals are used, lower heating rates produce more dissolution at temperatures between T_m and T_b and less dissolution at the final brazing temperature. Conversely, heating slowly when using thin filler metals produces less base metal dissolution (at any temperature) and negligible dissolution at the final brazing temperature. At very low heating rates, solidification can occur while heating from T_m to T_b.

I. INTRODUCTION

TRANSIENT liquid-phase (TLP) brazing involves a series of steps, namely, melting of the filler metal (at temperature T_m), heating to the final brazing temperature (T_b), base metal dissolution, isothermal solidification, and homogenization.[1] This paper models the TLP brazing process by treating base metal dissolution, isothermal solidification, and homogenization as one sequential process. Base metal dissolution is examined assuming that the heating rates from T_m to T_b range from 0.05 K/s to infinity. In this work, two brazing situations are considered, namely, constant liquid width (where liquid is continuously expelled throughout the brazing process) and variable liquid width (where the solid-liquid interface is able to move in an unrestricted manner throughout base metal dissolution).

II. BACKGROUND

The Nernst-Brunner theory of solid dissolution into liquid was derived based on the key assumptions that the liquid zone can be considered as a constant volume bulk

layer with a thin, constant thickness boundary film at the solid-liquid interface. Dissolution is determined by either the interface reaction or by the transport of material from the solid-liquid interface into the bulk liquid.[2]

Most experimental results support the idea that dissolution depends on transport processes, and that the interface reaction is not rate-controlling, except when high dissolution rates are promoted by forced stirring of the liquid. Lowell and Chalmers[3] theoretically examined the dissolution of solid in liquid and indicated that in an unstirred liquid system, movement of the solid-liquid interface was dependent on the square root of the holding time and that the boundary layer thickness also increased in a similar manner. In TLP brazing, the liquid can be considered to be unstirred because it is an extremely thin region.

Dissolution during TLP brazing has been examined in detail by Nakao et al.[4] and by Tuah-Poku et al.[5] Nakao et al.[4] developed a dissolution parameter based on the Nernst-Brunner theory; i.e., the dissolution rate of solid into liquid is given by the relation

$$C = C_{sat}[1 - \exp(-K(A/V)t]$$ [1]

where C = solute concentration in the liquid;
C_{sat} = solute concentration at saturation;
K = the dissolution rate;
V = volume of liquid;
A = area of solid-liquid interface; and
t = time.

Differentiating Eq. [1] gives

$$dc/dt = K(A/V)(C_{sat} - C)$$ [2]

H. NAKAGAWA, formerly Visiting Research Scientist, Department of Metallurgy and Materials Science, University of Toronto, is Research Instructor, Japan Welding Research Institute, Osaka University, Osaka, Japan. C.H. LEE, formerly Postdoctoral Fellow, Department of Metallurgy and Materials Science, University of Toronto, is Research Engineer, Research Institute of Industrial Science and Technology (RIST), Pohan, South Korea. T.H. NORTH, WIC/NSERC Professor, is with the Department of Metallurgy and Materials Science, University of Toronto, Toronto, M5S 1A4, ON, Canada.
Manuscript submitted September 28, 1989.

Assuming that the total amount of solute in the liquid is always constant, the dissolution parameter P^* is then given as

$$P^* = Kt = h[\ln (X_0\{X_t + ph\})/ph(X_0 - X_t)] \quad [3]$$

where P^* = the dissolution parameter;
X_t = the width of base metal dissolved at time t;
X_0 = the equilibrium (saturated) dissolution width;
p = the ratio of the liquid density to the solid density;
h = half of the initial liquid width;
K = constant; and
t = time.

The relation between the dissolution parameter and holding time was examined experimentally when brazing Ni-based superalloy material by using a Ni-Cr-B amorphous filler metal, and it was concluded that the Nerst-Brunner theory was applicable to dissolution during TLP brazing (Figure 1(a)). It is important to point out that in Nakao et al.'s experiments,[4] the width of the liquid layer was held constant throughout brazing. Conversely, Tuah-Poku et al.[5] studied dissolution of Ag base metal by using a copper filler metal in a configuration where the

(a)

(b)

Fig. 1—Relation between the dissolution parameter (P^*) and the holding time at different brazing temperatures (1373 K, 1398 K, and 1423 K) for (a) a constant liquid width during dissolution[4] and (b) an unrestrained liquid width during dissolution.[5]

liquid width was not held constant. Although they did not analyze their test results in terms of the Nerst-Brunner theory, recalculation by the present authors indicates that the relation between the dissolution parameter (P^*) and the brazing time is approximately parabolic in shape (Figure 1(b)). This would be expected if the interface motion was solute diffusion-controlled.

Any application of the Nerst-Brunner theory to TLP brazing has inherent problems. The thicknesses of liquid boundary films are approximately given by 2 to 3 $\sqrt{(Dt)}$, where D is the diffusion coefficient of solute in the liquid. Assuming diffusivity values in the range of 10^{-6} to 10^{-7} cm^2/s, a holding time of 100 seconds means that the diffusion layer thickness will be in the range of 70 to 300 μm. If the liquid width produced during TLP brazing is around 100 μm, the diffusion layer thickness will be of the same order of magnitude as the total liquid width. It follows that the Nernst-Brunner assumption of a thin boundary layer and a bulk liquid region is hardly applicable in TLP brazing operations. Also, the Nerst-Brunner theory has only been applied to, and confirmed experimentally, for binary systems. As a result, its extension to complex Ni-based superalloy/filler metal brazing situations may be questionable. Finally, Eq. [3] above neglects solute diffusion into the base metal, and it suggests that the time required for completion of dissolution (for X_t to equal X_0) will be infinite.

III. ASSUMPTIONS IN THE NUMERICAL MODEL

In complex fabrications, the width of the liquid melted can be held constant only in simple joint geometries, and the time for dissolution (and for isothermal solidification) will be much longer when the liquid layer is able to grow in an unrestricted manner. This paper models the effects of constant and unrestrained (variable) liquid width during base metal dissolution. In Nakao et al.'s experimental results[4] (Figure 1(a)), the slow rate of advance of the solid-liquid interface strongly suggests that dissolution during TLP brazing of Ni-based materials is dependent on solute diffusion, not on the interface reaction. this situation should apply except when an interface is covered with an oxide layer prior to brazing.[2] Liquid stirring will only be important when high-frequency induction heating is used to raise the components to the brazing temperature. In all other cases, convection can be neglected, and the key factor affecting base metal dissolution will be solute diffusion in the liquid.

The basic assumptions during modeling comprise the following:

(1) Use of a one-dimensional analysis involving a planar solid-liquid interface. No effect of grain-boundary penetration on the advance of the solid liquid interface is assumed.
(2) There is no convection or stirring in the liquid during dissolution (and subsequent isothermal solidification). This is reasonable when induction heating is not used. Also, it is assumed that there is no superheating or undercooling at the solid-liquid interface.
(3) The dissolution process is controlled by solute diffusion in liquid and solid and not by any interface reaction. Fick's law is applied in both liquid and solid phases.
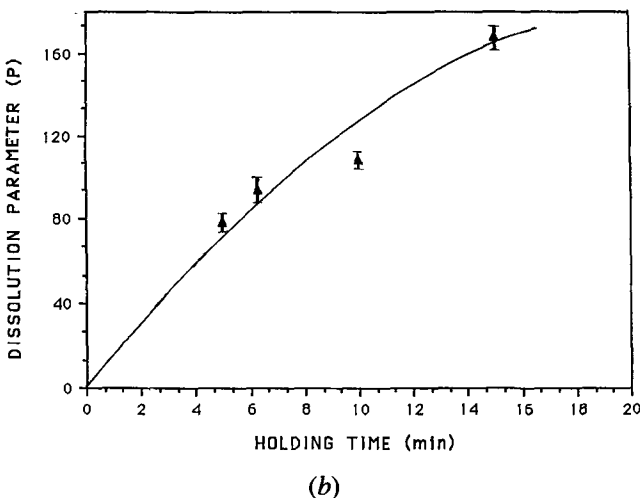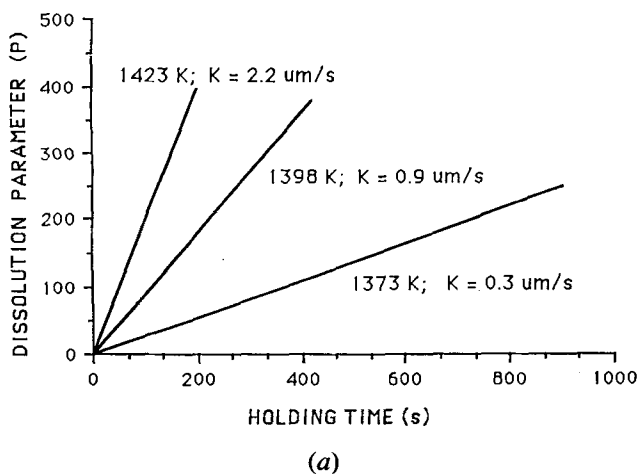
(4) The partition coefficient of the solute is independent of temperature.

(5) There is no effect of latent heat on the temperature distribution and on the rate of advance of the solid-liquid interface. This has been confirmed in preliminary calculations which considered the latent heat contribution.

(6) No volume change occurs during dissolution, and no second phases are formed during brazing.

The finite difference analysis considers that the solid-liquid interface moves in a stepwise manner. In effect, during dissolution, when the solute concentrations in the solid and liquid deviate from those given by equilibrium at any given temperature during a sudden advance, the interface halts until this deviation disappears. The details of this finite difference analysis are given in the Appendix.

IV. MATERIALS AND JOINING CONDITIONS EXAMINED

The base material was pure nickel. The filler metals were Ni-11 wt pct P and Ni-14 wt pct Cr-10 wt pct P filler metals having a eutectic temperature of 1153 K. The filler metal thicknesses ranged from 5 to 200 μm, and the heating rates (from T_m and T_b) varied from 0.05 K/s to infinity.

It is reasonable to assume that local equilibrium exists at the solid-liquid interface during dissolution. In effect, solute concentrations may be found using the liquidus and the solidus lines in the relevant equilibrium phase diagrams. In the Ni-P binary system, the gradient of the liquidus line is 52.3 K/wt pct.[6,7,8] However, only the solubility limit is available in the Ni-P binary diagram.[7] In an attempt to find a suitable partition coefficient for the Ni-P system, different partition coefficient values were used to calculate the time for completion of isothermal solidification and were compared to known experimental results given by Ikawa et al.[9] The use of a possible partition coefficient (1.54 × 10^{-2}) based on the ratio of the phosphorous concentrations at the solubility limit and at the eutectic point produced abnormally long calculated times compared to Ikawa et al.'s experimental results. The details of this comparison are presented in Reference 13. The partition coefficient of phosphorous in carbon steel solidifying as austenite has recently been measured as 0.13,[10] and use of this value in calculations of the time for completion of isothermal solidification during TLP brazing of Ni-based superalloys produced results close to those found by Ikawa et al.[9] (see Reference 13). As a result, this value was taken as the partition coefficient of phosphorous. The diffusivities of phosphorous in liquid and solid nickel were also not available, and the values for phosphorous in liquid and solid iron (austenite) were used in their place:[11,12]

in liquid: $D_{pl} = 1.35 \times 10^{-2}$

$$\exp(-23{,}700)\ [\text{cal/mol}]/RT\ [\text{cm}^2/\text{s}]$$

in solid: $D_{ps} = 0.01$

$$\exp(-43{,}700)\ [\text{cal/mol}]/RT\ [\text{cm}^2/\text{s}]$$

where R is the gas constant and T is absolute the temperature.

V. RESULTS AND DISCUSSION

The detailed modeling results can be conveniently handled by considering the different effects of assuming an infinite and a finite heating rate between the temperatures T_m and T_b.

A. Dissolution Assuming an Infinite Heating Rate between T_m and T_b

As indicated previously, there are two possible situations which can arise in TLP brazing, namely, where there is an unrestrained (variable) liquid width during brazing and where there is a constant liquid width due to expulsion of excess liquid throughout the dissolution process. These will be discussed separately.

1. Assuming an unrestricted liquid width during brazing

Figure 2 shows the phosphorous distribution in solid and liquid nickel when brazing at 1473 K assuming that the liquid width is variable (unrestrained). The abscissa is distance divided by half the thickness of the filler metal (and this normalization is applicable irrespective of the filler metal thickness considered). The phosphorous distribution in the liquid is not uniform (particularly in the early stages of brazing), and the diffusion layer is large in comparison with the liquid width produced during brazing. The time for completion of dissolution depends on the square of the filler metal thickness, and the amount of phosphorous diffusion into solid nickel is limited, even in the final stages of the dissolution period. However, it should be pointed out that although phosphorous diffusion into the base metal is limited, it does play an important role in calculations determining the time for completion of dissolution (Section B). It is also clear from Figure 2 that the phosphorous concentration profile in the liquid is such that dissolution during TLP brazing cannot be adequately examined using an extension of the Nernst-Brunner theory, even for an infinite heating rate between T_m and T_b (since the thin boundary layer and constant volume bulk liquid requirements are not met).

Figure 3 shows the relation between holding time and the advance of the solid-liquid interface at various bonding temperatures for a 200-μm-thick filler metal. The solid circle on this diagram is the point at which dissolution is completed at any temperature. It follows that the finite difference model overcomes Eq. [1]'s basic limitation (it cannot be used to calculate the time required for completion of dissolution). Increasing temperature increases the rate of advance of the solid-liquid interface (since the diffusion rate in the liquid is higher, and the difference between the eutectic concentration and the equilibrium liquidus temperature is much greater). The time required for dissolution shows a minimum at 1423 K. This occurs since the time for completion depends on the maximum liquid width, and this increases with increasing brazing temperature (Figure 4). However, increased solute diffusivity at higher temperatures tends to decrease the time for completion of the dissolution stage so there is competition between these two factors. It was previously noted that the time dependence of the advance of dissolution is related to the square of the filler metal thickness. However, this does not mean
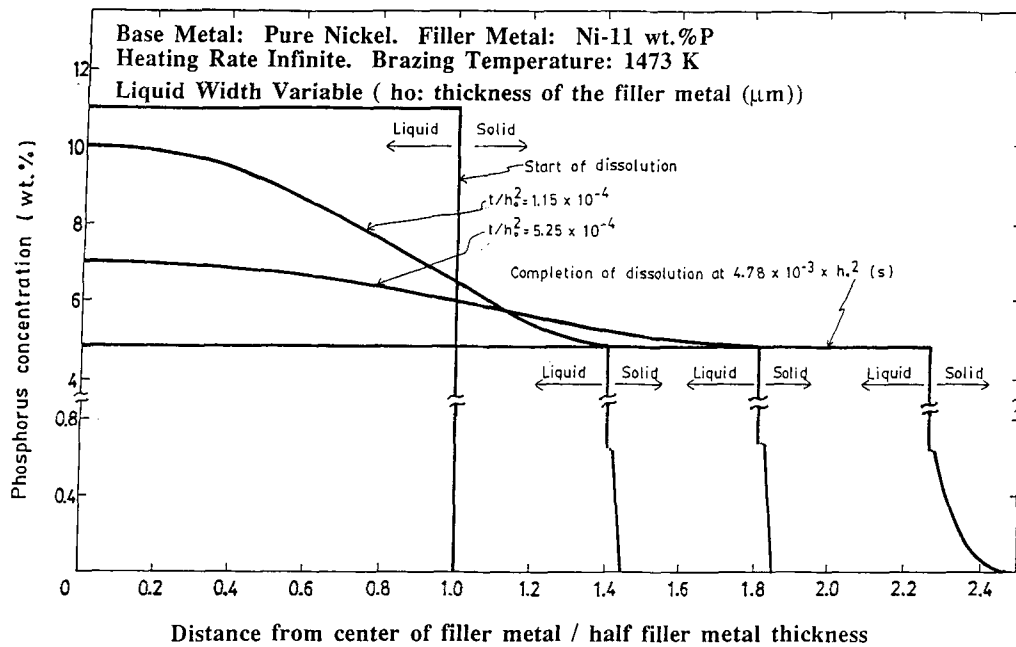
Fig. 2 — Phosphorous distribution in solid and liquid nickel at 1473 K (assuming an unrestrained liquid width during dissolution and an infinite heating between T_m and T_b).

that the solid-liquid interface moves proportionally with the square root of the holding time (Figure 5). The solid-liquid interface advances in proportion to the square root of the holding time only in the early stages of the brazing process.

The solute diffusivity in the liquid markedly affects the rate of advance of the solid-liquid interface. In this

work, the diffusivity value used is that evaluated for Fe-1.1 pct P in the temperature range of 1673 to 1873 K,[11] and these temperature values are higher than in conventional brazing. The influence of phosphorous diffusivity on the rate of advance of the solid-liquid interface is highlighted in Figure 6, where three different diffusivity values are considered, namely, 1.0×10^{-6} cm^2/s, 2.0×10^{-6} cm^2/s, and 4.0×10^{-6} cm^2. Low solute diffusivity values decrease the rate of advance of the solid-liquid interface, particularly in the final stages of the dissolution process. For a fixed advance by the solid-liquid interface, the time differences (after the initiation of the dissolution process) are approximately doubled, except in the final stages of the dissolution process. This large time difference during the final stage of the dissolution
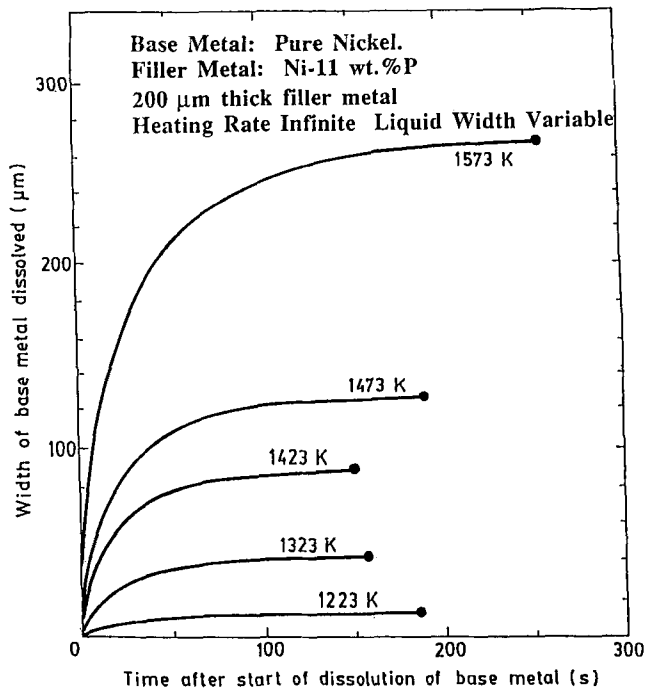

Fig. 3 — Relation between holding time and the advance of the solid/liquid interface at a range of bonding temperatures (for a 200-μm-thick filler metal, an unrestrained liquid width, and an infinite heating rate between T_m and T_b). The "●" mark on each curve indicates the point at which dissolution is complete.
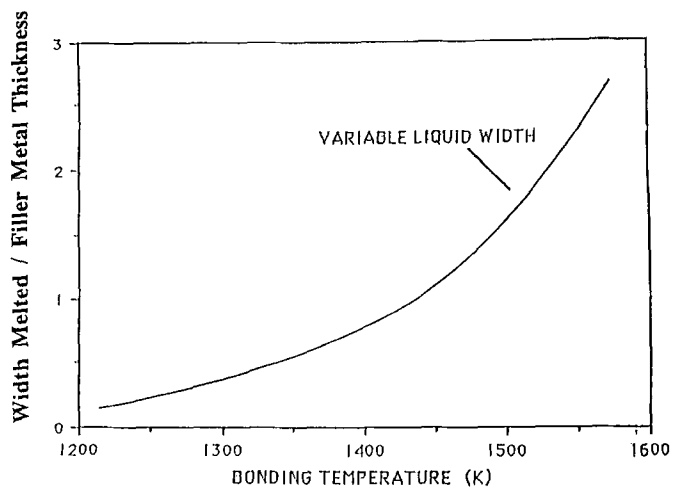

Fig. 4 — Relation between temperature and the maximum liquid width produced during brazing (assuming an unrestrained liquid width during dissolution and an infinite heating rate between T_m and T_b).
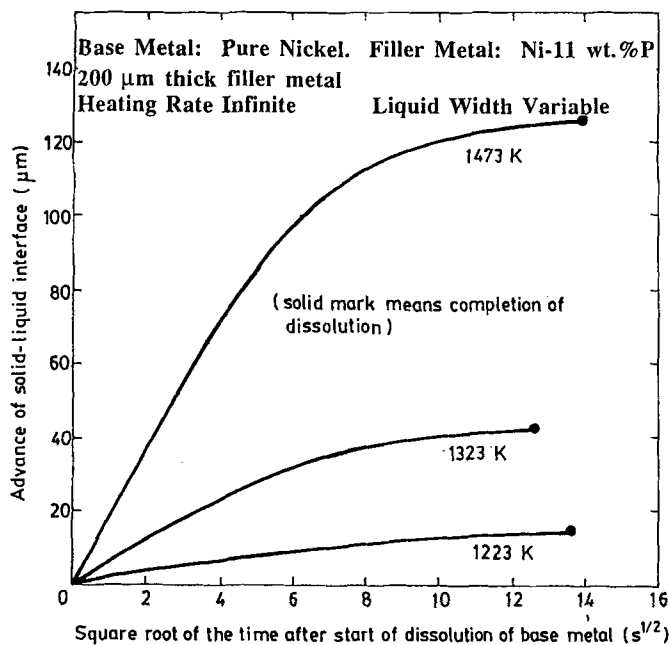
Fig. 5—Relation between the advance of the solid/liquid interface and the holding time (assuming an unrestrained liquid width during dissolution and an infinite heating rate between T_m and T_b).

process depends on the interplay of solute diffusion in the liquid and solute diffusion into the base metal. The solute concentration required for local equilibrium at the solid-liquid interface is supplied by solute diffusion in the liquid. If solute diffuses into the base metal, this will decrease the solute concentration at the solid-liquid interface and therefore decrease the advance of the interface. This emphasizes the important role of solute dif-

fusion into the base metal on the time required for the transition from dissolution to isothermal solidification. In this connection, it is the neglect of solute diffusion into the base metal that makes Eq. [3] predict an infinite value for the completion of dissolution.

As mentioned previously, a phosphorous partition coefficient value of 0.13 was employed in all calculations, and the use of a value of 1.54×10^{-2} produced completion times (for isothermal solidification) which greatly exceeded experimental values. It must be emphasized that this difference in partition coefficient values (from 1.54×10^{-2} to 0.13) only produced a 5 pct change in the time required for completion of dissolution.

2. *Assuming a constant liquid width during brazing*

The phosphorous distribution in liquid and solid during dissolution at 1473 K is shown in Figure 7. In this figure, the abscissa are presented in terms of distance divided by half the filler metal thickness, and holding time is presented as a function of the square of the filler metal thickness. The phosphorous concentration profile is nonuniform, and its shape indicates that application of the Nernst-Brunner theory to TLP brazing is unreasonable. These results also show that the time for completion of dissolution depends on the square of the filler metal thickness and that diffusion of solute into the base metal is negligible, except in the final stages of dissolution.

Figure 8 shows the relation between the holding time required for dissolution and brazing temperature for a 200-μm-thick filler metal. The solid circles indicate completion of the dissolution process, and it is clear that increasing brazing temperature decreases the time required for completion of dissolution. This effect of brazing temperature correlates well with Nakao *et al.*'s experimental results when brazing Ni and Ni-based superalloys using Ni-P filler metal.[4] This decrease in
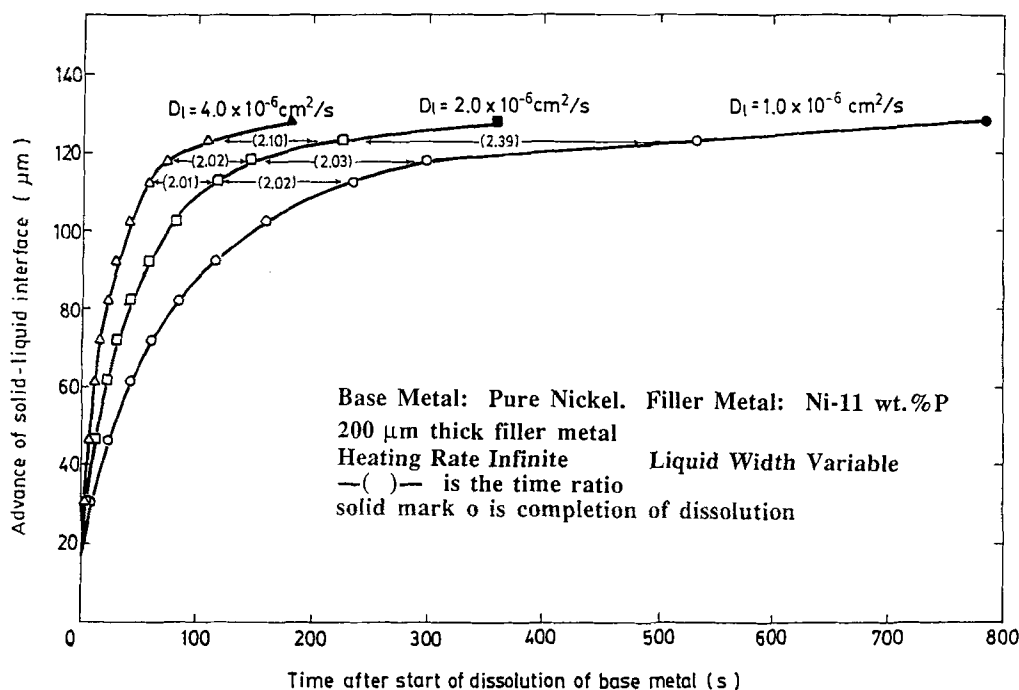

Fig. 6—Effect of phosphorous diffusivity on the rate of advance of the solid/liquid interface (assuming an unrestrained liquid width during dissolution and an infinite heating rate between T_m and T_b).
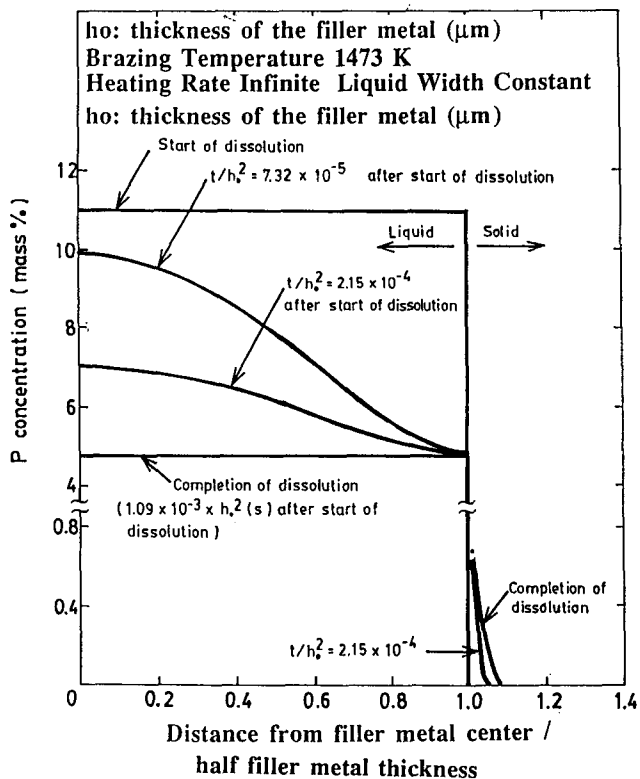
Fig. 7—Phosphorous distribution in liquid and solid nickel at 1473 K (assuming a constant liquid width during brazing and an infinite heating rate between T_m and T_b).
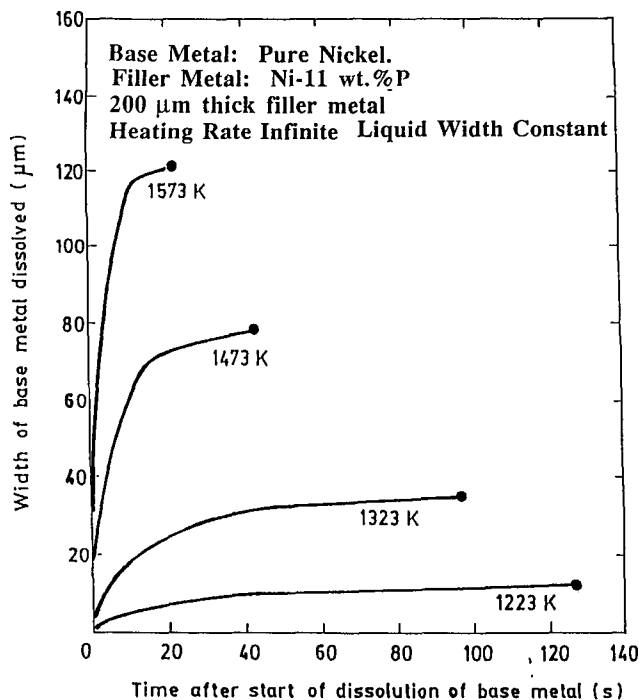
dissolution time at higher brazing temperatures is due to increased phosphorous diffusion rates. It is apparent that the time for completion of dissolution in Figure 8 is much shorter than that in Figure 3, since the expelled liquid is much higher in phosphorous content than the equilibrium concentration at the solid-liquid interface. Figure 9 compares the liquid width/brazing temperature relations for constant and variable (unrestrained) liquid width situations. The difference in dissolution width is largest at high brazing temperatures; e.g., at 1573 K, it is almost 2.5 times larger when an unrestrained liquid width brazing situation is considered.

Figure 10 shows the relation between holding time and the dissolution parameter P^* (from Eq. [3]) for variable and constant liquid width situations. This particular relation is not linear at any brazing temperature when the liquid width is unrestrained (variable). It is almost linear when the liquid width is maintained constant during brazing operations, except in the very early stages and in the final stages of the dissolution process. However, it should be emphasized that although Figure 10 suggests some linear correlation between holding time and the dissolution parameter (P^*) over a given range, this cannot be taken as confirmation that the Nernst-Brunner theory can be applied to TLP brazing situations. For example, Figures 2 and 7 clearly indicate that the phosphorous concentration profile in the liquid confirms that conditions are far from those required by the Nerst-Brunner theory (no bulk liquid region or constant dimension boundary layer exists).

B. Dissolution Assuming a Finite Heating Rate between T_m and T_b

When the TLP brazing process was first envisaged, the assumption was made that the heating rate from the melting temperature (T_m) of the filler metal to the bonding temperature (T_b) was infinite (Figure 11). In effect, the concentration of the melting point depressant in the liquid phase (after melting of the filler metal) is constant during the heating stage from T_m to T_b. This is the vertical line ab in Figure 11. This idea implies that base metal dissolution does not occur during heating and that
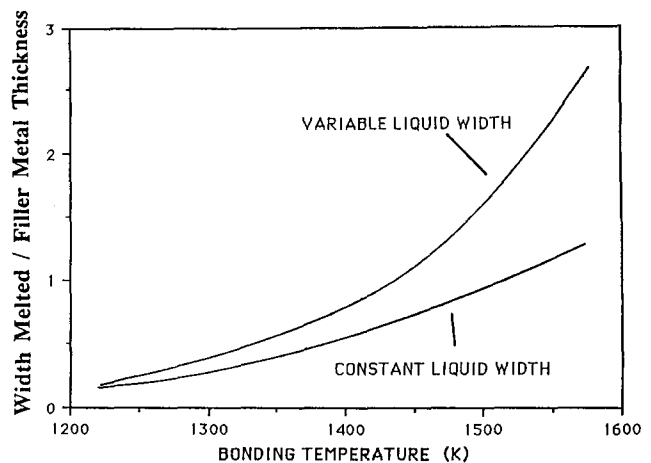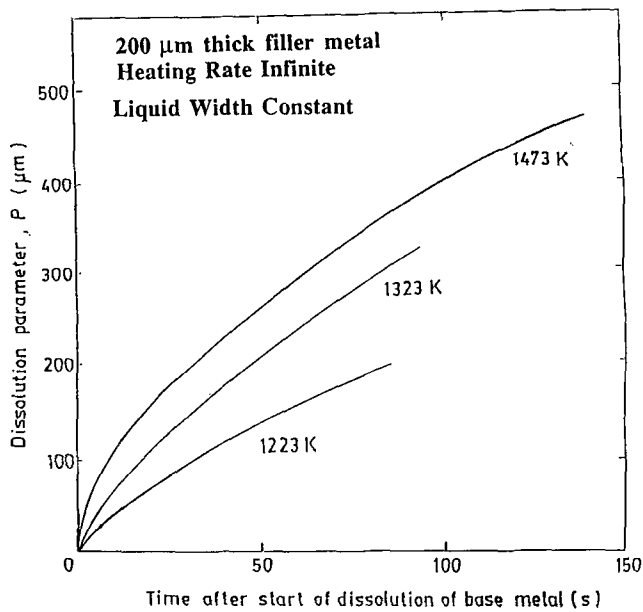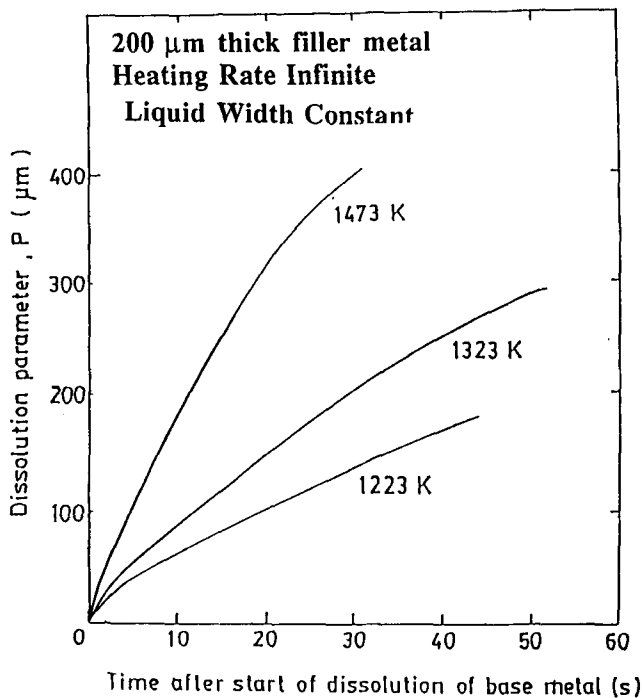

Fig. 8—Relation between holding time and the advance of the solid/liquid interface at a range of temperatures (assuming a constant liquid width during brazing for a 200-μm-thick filler metal and an infinite heating rate between T_m and T_b).

Fig. 9—Relation between the width of base metal dissolved and temperature for constant and unrestrained liquid width situations.

Fig. 10—Relation between holding time and the dissolution parameter (P^*) and (a) an unrestrained liquid width situation and (b) a constant liquid width situation (assuming an infinite heating rate between T_m and T_b).
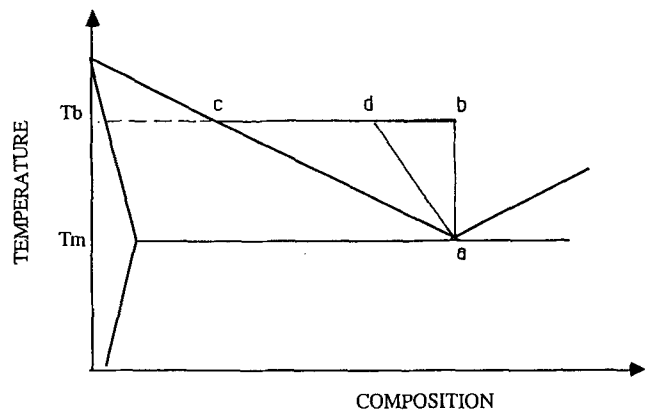

Fig. 11—Schematic representation of the TLP brazing process.

to diffuse into the base metal, and this will decrease the amount of base metal dissolution that occurs during brazing, especially when thin filler metals are used. In addition, if there is sufficient solute diffusion into the base metal, the relationships between dissolved width (normalized with respect to filler metal thickness) and dissolution time (normalized with respect to the square of the filler metal thickness), which were determined for an infinite heating rate, may not apply. It is even possible that very slow heating rates will promote solidification during the heating cycle from T_m to T_b.

Figure 12 shows the phosphorous distributions in liquid and solid at a brazing temperature of 1400 K, assuming a variable (unrestrained) liquid width condition, a heating rate of 50 K/s, and filler metal thicknesses ranging from 5 and 200 μm. The origin on the abscissa of Figure 12 is the center of the filler metal. The scale on the abscissa is selected so that the initial position of the solid-liquid interface is the same for both filler metal thicknesses. The phosphorous distribution in the liquid is almost uniform for the 5-μm-thick filler metal). In contrast, a significant phosphorous concentration profile is exhibited in the case of the 200-μm-thick filler metal.

the solute concentration in the liquid changes along the path bc at the brazing temperature (Figure 11). However, an infinite heating rate from temperature T_m to T_b is not really applicable to conventional fabrication situations.

When the heating rate between T_m and T_b is finite, the solute concentration may change along the line ad in Figure 11, as an example. Also, as the heating rate decreases, the melting point depressant will have more time
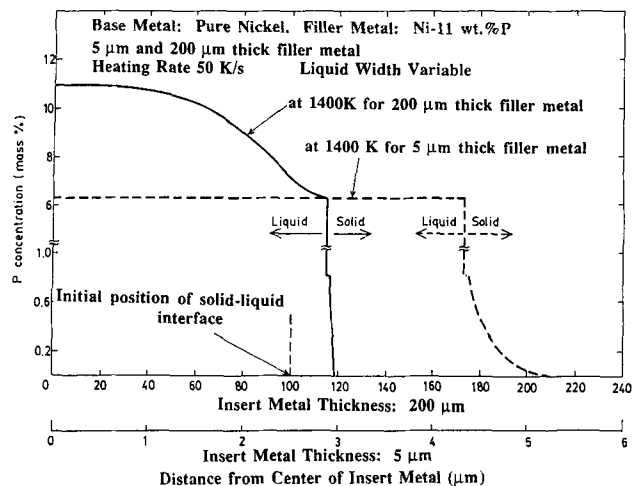

Fig. 12—Phosphorous distribution in liquid and solid nickel at 1400 K (assuming an unrestrained liquid width, filler metal thicknesses from 5 to 200 μm, and a heating rate between T_m and T_b of 50 K/s).

Figure 13 shows the average phosphorous concentrations in the liquid at a range of heating rates (for 5- and 200-μm-thick filler metals). Decreasing the heating rate in the case of 200-μm-thick filler metal shifts the curves to the left (to lower phosphorous concentration) on the diagram, and at a heating rate of 1 K/s, the phosphorous concentration nearly follows the liquidus line in the Ni-P equilibrium diagram. When a 5-μm-thick filler metal is considered, the liquidus line is followed for heating rates less than 50 K/s. This shift in the liquid phosphorous concentration/temperature relation with heating rate and filler metal thickness is illustrated in Figure 14. The results in Figure 12 and 13 were calculated assuming that the liquid width was unrestrained. Similar results were produced when a constant liquid width situation was modeled.

Although Figure 12 considers dissolution when using a 200-μm-thick filler metal, the typical thicknesses of brazing filler metals are much smaller than this value (around 50 μm). Similarly, heating rates of 50 K/s may be difficult to achieve except in laboratory situations, and thus, the concentration of the melting point depressant in the liquid will deviate considerably from line *ab* in Figure 11. This deviation from the idealized filler metal melting assumption (*ab* in Figure 11) can be assessed for any given set of filler metal thickness, temperature, and heating rate conditions. The degree of uniformity of solute diffusion during dissolution can be estimated by using the homogenizing index (z); *i.e.*,

$$z = L/\sqrt{D_{pl}t} \qquad [4]$$

where L is the size of the zone in the liquid where diffusion occurs, D_{pl} is the diffusivity, and t is the time. If
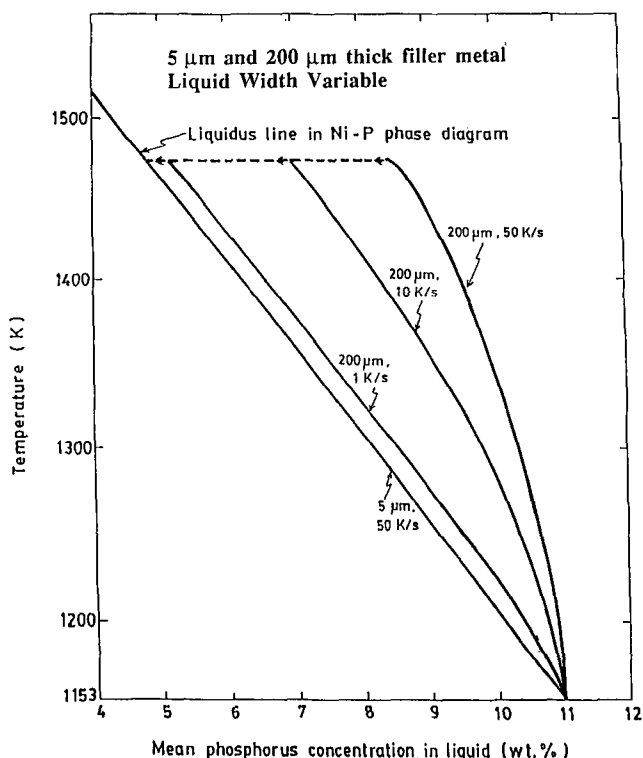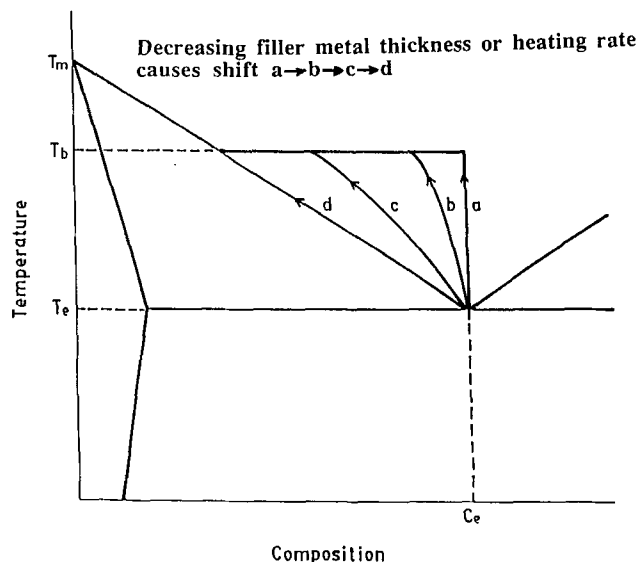

Fig. 14—Effect of decreasing heating rate or filler metal thickness on the liquid composition during TLP brazing.

the maximum width of liquid (X_m) in previously calculated results (Figure 4) is taken as L and if the diffusivity at a temperature midway between temperature T_m and T_b is taken as D_{pl}, then the value of t in Eq. [4] can be expressed as

$$t = (T_b - T_m)/R_h \qquad [5]$$

where R_h is the heating rate. It follows that Eq. [4] becomes

$$z = L/\sqrt{\{(T_b - T_m)D_{pl}/R_h\}} \qquad [6]$$

The different temperature-composition paths a, b, c, and d during the heating cycle from T_m to T_b (Figure 14) can be described using a distribution index (α); *i.e.*,

$$\alpha = [(C_{lM} - C_{leq})/(C_e - C_{leq})] \times 100 \text{ (pct)} \qquad [7]$$

where C_e is the eutectic concentration and C_{lM} and C_{leq} are the maximum in liquid at a given temperature and the equilibrium liquidus concentration, respectively. α has a maximum value at the eutectic temperature and decreases with increase in temperature. Figure 15 shows the relation between z and α in the temperature range of brazing operations (1323 and 1473 K), for various filler metal thicknesses and heating rates ranging from 0.1 to 100 K/s. When z is less than 0.3, the value of α is less than 0.1, and the solute concentration in the liquid nearly follows the liquidus line.

The influence of heating rate on the advance of the solid-liquid interface is shown in Figure 16 for a 200-μm-thick filler metal. The amount of base metal dissolved at temperatures between T_m and T_b and at the brazing temperature T_b depends on the heating rate. When the heating rate decreases, more base metal is dissolved at temperatures below T_b, and the amount of dissolution at T_b is less. For 5-μm-thick filler metal brazed at heating rates from 0.05 to 50 K/s, more base metal is dissolved as temperature rises, but there is negligible dissolution at T_b (Figure 17). At very low heating rates (0.05 to 0.5 K/s), the movement of the solid-liquid
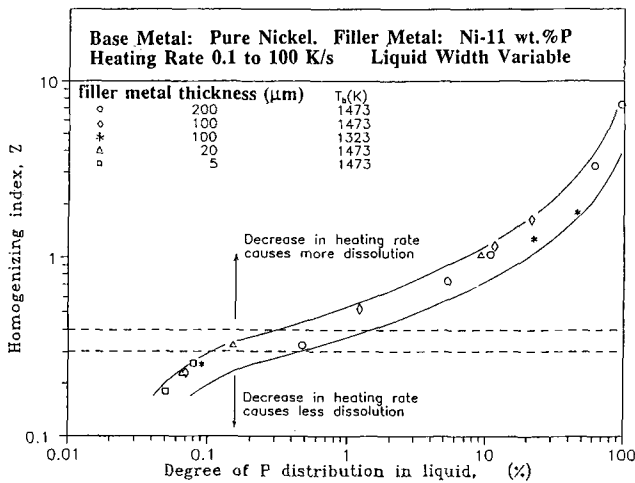

Fig. 13—Average phosphorous concentrations in liquid at a range of heating rates (for 5- and 200-μm filler metal thicknesses).

Fig. 15—Relation between the homogenizing index (z) and distribution index (a) for a range of heating rates and filler metal thicknesses.

Fig. 17—Effect of heating rate on the advance of the solid/liquid interface (for a 5-μm-thick filler metal and an unrestrained liquid width situation).

interface is affected by solidification which occurs during the heating cycle. This solidification effect is markedly dependent on the diffusivity of the melting point depressant. If the melting point depressant had a much higher diffusivity value than phosphorous (e.g., boron), this solidification effect would be even more pronounced.

It is also apparent from Figure 17 that the use of thin filler metals and slow heating rates will decrease the amount of base metal dissolved at any given temperature. The differences between Figures 16 and 17 can be explained as follows:

(1) Thick filler metal: In this case, the phosphorous concentration profile in the liquid is not uniform (Figure 12), and solute diffusion from the liquid to the solid-liquid interface is the main driving force for dissolution. It follows that a slower heating rate will produce more base metal dissolution in the temperature range between T_m and T_b.
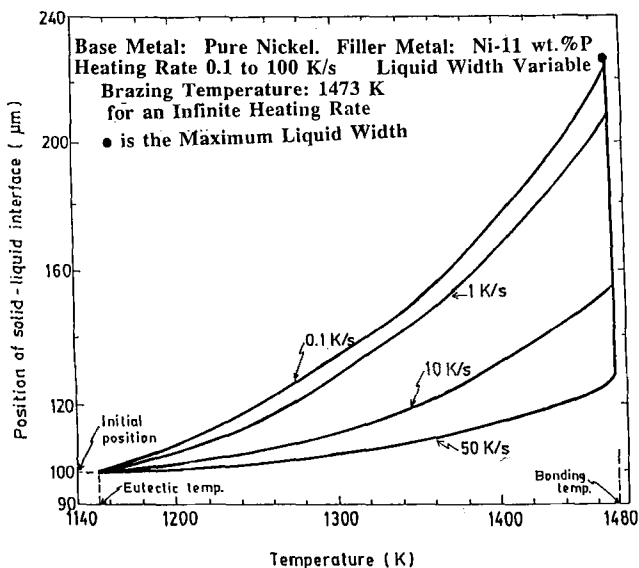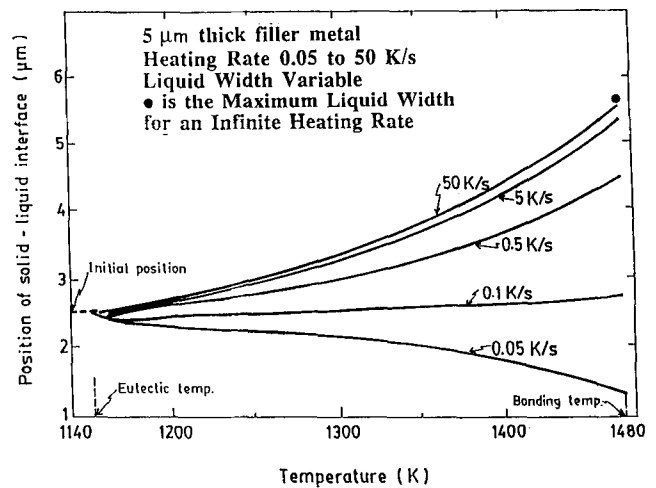

Fig. 16—Effect of heating rate on the advance of the solid/liquid interface at a brazing temperature of 1473 K (for a 200-μm-thick filler metal and an unrestrained liquid width situation).

(2) Thin filler metal: In this case, the concentration profile in the liquid is uniform (Figure 12), and an increase in temperature is the prerequisite for further advance of the solid-liquid interface. This explains why no dissolution occurs at the final brazing temperature. A temperature change from T_1 to T_2 produces a concentration change from C_{l1} to C_{l2} during an infinitesimal time interval, t_1 to t_2 (Figure 18(a)), and the resultant advance is illustrated in Figure 18(b). The dotted area A_1 must equal that of area A_2 plus the diffused area A_d. Lowering the heating rate will increase A_d and thus decrease A_2; i.e., there will be less dissolution. However, if $A_d > A_1$, then area A_2 will be negative and solidification will occur when heating between T_m and T_b. The transition from thick to thin filler metal melting characteristics can be estimated using the z or a parameters, and the critical condition will occur when z is around 0.3 and α is around 0.1 (Figure 15). Also, a low heating rate will allow considerable diffusion of solute into the base metal, and this will markedly influence the isothermal solidification process that immediately follows dissolution. This effect is examined in detail in Reference 13.

C. Dissolution When Using Ternary Ni-Cr-P Filler Metals

The influence of chromium and phosphorous in combination on dissolution behavior during TLP brazing was examined by examining brazing with two different filler metal chemistries (Ni-11 wt pct P and Ni-14 wt pct Cr-10 wt pct P). These alloys have identical eutectic temperatures. In these calculations, the partition coefficient and liquidus gradient values in the Ni-Cr binary system were taken as 0.887 and 2.1 K/wt pct.[8] The diffusivity of Cr in solid Ni was calculated by using the relation[14]

$$D_{Crs} = 1.1 \exp(-65,000 \text{ [cal/mol]}/RT) \quad \text{[cm}^2\text{/s]}$$

Since the diffusivity of chromium in liquid nickel is not available in the literature, two values were examined for calculation purposes, that of phosphorous in liquid and one quarter of this value. When the phosphorous and
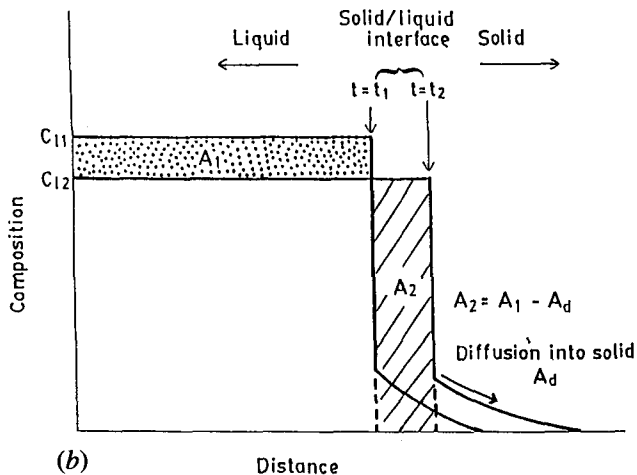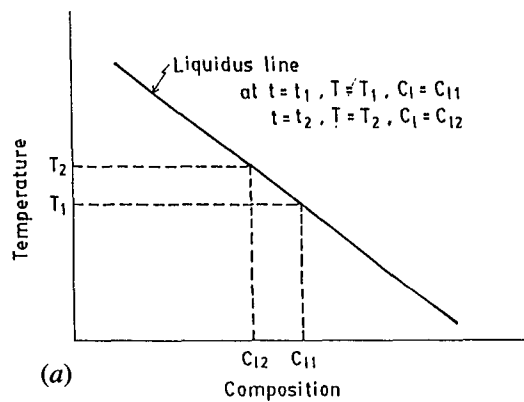
Fig. 18—(a) and (b) Schematic representation of liquid and solid phosphorous concentrations during an infinitesimal advance of the solid/liquid interface (for a thin filler metal when the heating rate is slow).

be much longer than that when using a simple Ni-B filler metal chemistry. Also, Table II shows the effect of chromium content in the base metal on the time required for completion of dissolution, based on the assumption that the diffusivities of phosphorous and chromium in the liquid are identical. It is apparent that an increase in base metal chromium content increases both the liquid width (possibly due to a melting point depressant effect) and the time required for completion of dissolution.

Based on the above argument, it is suggested that the time required for completion of dissolution during TLP brazing of complex commercial superalloys will be increased due to the presence of elements other than the melting point depressant in the base metal or filler metal. This might explain the very long dissolution times observed when commercial Ni-based superalloys were brazed by using a boron-containing filler metal.[4]

VI. CONCLUSIONS

Detailed modeling of dissolution during TLP brazing of Ni by using Ni-11 wt pct P and Ni-14 wt pct Cr-10 wt pct P filler metals has indicated the following.

A. Assuming an Infinite Heating Rate between T_m and T_b

1. Constant liquid and variable (unrestrained) liquid width brazing conditions produce different times for completion of the dissolution process. Since it is difficult to control the liquid width in complex fabrication geometries, it is likely that unrestrained liquid width

chromium diffusivities are identical, the time for completion of the dissolution process is within 7 pct of that when using a simple Ni-11 pct P filler metal. However, if the diffusivity of chromium is taken as one quarter that of phosphorous, the time for completion of dissolution is 1.4 times as great as in the Ni-P filler metal case (Table I). If a high-diffusivity melting point depressant such as boron was used in the filler metal, the diffusion rate of this element would certainly be much faster than that of substitutional elements. Consequently, the dissolution time when using a Ni-Cr-B filler metal would

Table I. Effect of Chromium Diffusivity in the Liquid on the Time Required for Completion of Dissolution during Transient Liquid-Phase Brazing with Different Base Metal/Filler Metal Combinations

Base Metal	Filler Metal	$2X_M$* (μm)	Heating Rate
Pure Ni	Ni-11 pct P	11.10	infinite
Pure Ni (assuming the diffusivity of P and Cr are identical)	Ni-14 pct Cr	11.90	infinite
Pure Ni (assuming the diffusivity of Cr is one quarter of P)	Ni-14 pct Cr-10 pct P	15.54	infinite

*$2X_M$ is the maximum liquid width produced during dissolution.

situations will occur, and this will markedly affect the optimum brazing cycle required for joining.

2. For both constant and unrestrained liquid width conditions, the time required for completion of dissolution is proportional to the square of the filler metal thickness, and the advance of the solid-liquid interface is approximately related to the inverse of the square root of the solute diffusivity in the liquid, except in the final stages of the dissolution process. Although phosphorous diffusion into the base metal is limited, it is important in calculations which determine the time required for completion of dissolution.
3. The essential requirement for application of the Nernst-Brunner theory, that bulk liquid exists with a thin boundary layer, is not supported by calculations that assume an infinite heating rate between the filler metal melting point, T_m, and the brazing temperature, T_b.
4. The diffusion rate of phosphorous in liquid has a large influence on the rate of advance of the solid-liquid interface during dissolution, but the partition coefficient of the solute has little effect on this parameter.
5. When a multicomponent filler metal composition (Ni-14 wt pct Cr-10 wt pct P) is used, the time for completion of dissolution is longer than that when using a simple binary Ni-11 wt pct P filler metal composition.

B. *Assuming a Finite Heating Rate between T_m and T_b*

1. The dissolution behavior that was modeled when assuming an infinite heating rate between the filler metal melting point and the brazing temperature (dissolution width normalized by the filler metal thickness and dissolution time normalized by the square of the filler metal thickness) was not followed when a finite heating rate was applied.
2. As the heating rate or the filler metal thickness is decreased, the phosphorous concentration in the liquid tends to follow the liquidus line. This tendency can be estimated by using the homogenizing index (z) which combines the effects of filler metal thickness, diffusivity in the liquid, brazing temperature and heating rate, and a distribution index α. The transition from thick to thin filler metal melting characteristics occurs when z is around 0.3 and α is around 0.1.
3. For thick filler metals (around 200 μm), lower heating rates produce more dissolution at any given temperature and less dissolution at the final brazing temperature. However, the dissolved width is almost unchanged for heating rates ranging between 0.1 and 100 K/s and is similar to that produced when an infinite heating rate between T_m and T_b is assumed. This behavior was explained by the nonuniform phosphorous concentration profile present in the liquid.
4. For thin filler metals (around 5 μm), lower heating rates produce less base metal dissolution (at any temperature) and negligible dissolution at the brazing temperature due to the uniform phosphorous concentration in the liquid and to solute diffusion into the base metal. At very low heating rates, solidification can occur when heating from the filler metal melting point to the final brazing temperature.

APPENDIX
Details of the numerical analysis

This program involved explicit forward finite difference modeling. The approach used in this work is similar to that published by Matsumiya.[15]

A. *Coordinate System Employed*

Half of the filler thickness is divided into N_d (5 to 20) meshes, each of width ΔX, except for mesh point 1, which had a width $\Delta X/2$. Meshes 2 to $4N_d$ had width ΔX; from $4N_{d+1}$ to $6N_d$ they had width $5\Delta X$. Those from $6N_{d+1}$ to $8N_d$ had widths of $25\Delta X$, and those from $8N_{d+1}$ to $12N_d$ had widths of $125\Delta X$. It follows that the analysis matrix was 620 times as large as half the thickness of the filler metal. The coordinate system employed during finite difference modeling is shown in Figure 1A.

B. *Stepwise Advance of the Interface*

Fick's second law was solved numerically by repeating a procedure of sudden advance of the solid-liquid interface followed by a transitory pause. This is shown schematically in Figure 2A (*i.e.*, Figure 2A(a) just before an advance and Figure 2A(b) just after an advance). For any advance, the conservation of mass requires

$$C_l(i) + C_s(i + 1) = C_{sb}(i + 1) + C_{sb}(i + 2) \quad [1]$$

where the subscript b applies to just before the advance and i refers to the mesh located in the liquid just at the solid-liquid interface. However, for local equilibrium,

$$C_s(i + 1) = kC_l(i) \quad [2]$$

Fig. 1A—Coordinate system used during finite difference modeling.

Dissolution of base metal

(a) Just before advance of
solid-liquid interface
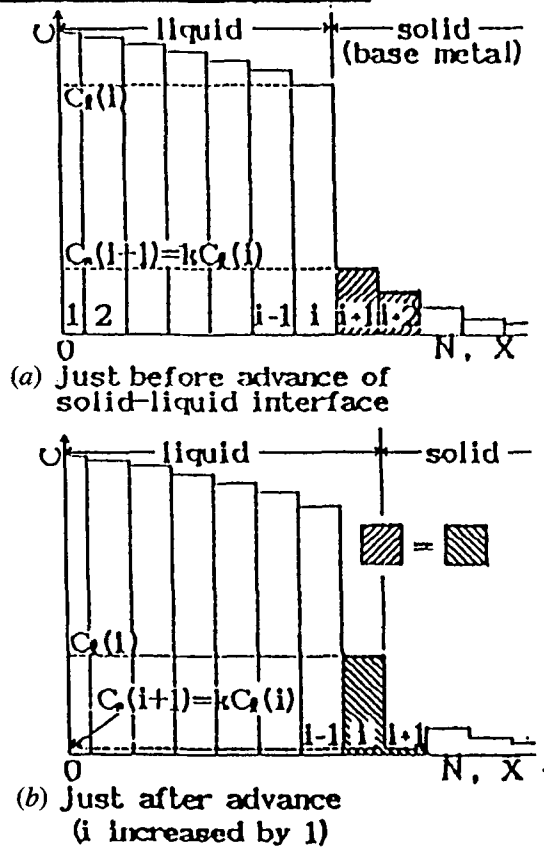
(b) Just after advance
(i increased by 1)

Fig. 2A—Solute distribution during dissolution (a) just before an advance of the solid/liquid interface and (b) just after an advance of the solid/liquid interface.

where k is the partition coefficient of the solute. From Eqs. [1] and [2], we have

$$C_l(i) = [C_{sb}(i + 1) + C_{sb}(i + 2)]/(1 + k) \qquad [3]$$

$$C_s(i + 1) = k[C_{sb}(i + 1) + C_{sb}(i + 2)]/(1 + k) \qquad [4]$$

In the computer program, $C_{sb}(i + 1)$ and $C_{sb}(i + 2)$ in Eqs. [1], [3], and [4] are expressed as $C_{sb}(i)$ and $C_{sb}(i + 1)$, since i increases by one at the moment of advance of the solid-liquid interface.

During isothermal solidification, the solute distribution just before and just after the sudden retreat of the solid-liquid interface was examined as follows. The concentrations in the liquid and solid at the interface are given by the equations:

$$C_l(i) = [C_{lb}(i - 1) + C_{lb}(i)]/(1 + k) \qquad [5]$$

$$C_s(i + 1) = k[C_{lb}(i + 1) + C_{lb}(i)]/(1 + k) \qquad [6]$$

In the computer program, $C_{lb}(i - 1)$ and $C_{lb}(i)$ in Eqs. [5] and [6] are expressed as $C_{lb}(i)$ and $C_{lb}(i + 1)$ since i decreases by one at the moment of retreat of the solid-liquid interface.

C. Transitory Pause of the Solid-Liquid Interface

The concentration values expressed in Eqs. [3] through [6] deviate from those in equilibrium at the brazing temperature (during a sudden advance or retreat of the solid-

liquid interface). As a result, the interface will suffer a transitory phase until this deviation disappears. After this difference in solute concentration disappears, the solid-liquid interface again advances. The explicit finite difference method calculates the solute distribution during this transitory pause by analyzing Fick's second law. The above equations can be expressed containing D_l and D_s as the diffusivities of the solute in the liquid and in the solid and Δt as the time interval which prevents any divergence in the calculated result; i.e., for mesh point 1 in the liquid,

$$C_l(1) = C_{lb}(1) + 2D_l[C_{lb}(2) - C_{lb}(1)] \, \Delta t/\Delta X_i^2 \qquad [7]$$

For a general mesh point in the liquid,

$$C_l(n) = C_{lb}(n) + D_l[(C_{lb}(n + 1)$$
$$- 2C_{lb}(n) + C_{lb}(n - 1)]\Delta t/\Delta X_i^2 \qquad [8]$$

For mesh points i and $i + 1$,

$$C_l(i) = C_{lb}(i) + D_l[C_{lb}(i - 1) - C_{lb}(i)]$$
$$\cdot \Delta t/\Delta X_i^2/(1 + k)$$
$$+ D_s[C_{lb}(i + 2) - C_{sb}(i + 1)]$$
$$\cdot \Delta t/\Delta X_i^2/(1 + k) \qquad [9]$$

$$C_s(i + 1) = kC_l(i) \qquad [10]$$

For a general mesh in the solid,

$$C_s(n) = C_{sb}(n) + D_s[C_{sb}(n + 1) - 2C_{sb}(n)$$
$$+ C_{sb}(n - 1)] \, \Delta t/\Delta X_i^2 \qquad [11]$$

In these equations, ΔX is ΔX_i if n is less than or equal to 100 or ΔX_2 if n is greater than 100.

D. Determination of Liquidus Temperature

The liquidus temperature at the solid-liquid interface (T_{li}) is calculated using the relation

$$T_{li} = T_m + G_l[C_e - C_{l(i)}] \qquad [12]$$

where T_m is the eutectic temperature, G_l is the liquidus gradient in the liquid, C_e is the phosphorous content at the eutectic point, and $C_{l(i)}$ is the phosphorous concentration in the liquid at the interface.

In the case of a ternary system, the liquidus temperature is calculated from the relation

$$T_{li} = T_e + G_{l1}[C_{e1} - C_{l1(i)}]$$
$$+ G_{l2}[C_{e2} - C_{l2(i)}] \qquad [13]$$

where G_{l2} is the liquidus gradient in the liquid due to chromium, C_{e1} and C_{e_2} are the eutectic concentrations in the case of the Ni-Cr-P ternary, and $C_{2(i)}$ is the chromium content in the liquid at the interface.

E. Transition from Dissolution to Isothermal Solidification

The transition from dissolution to solidification occurs when the liquidus temperature at the interface diverges
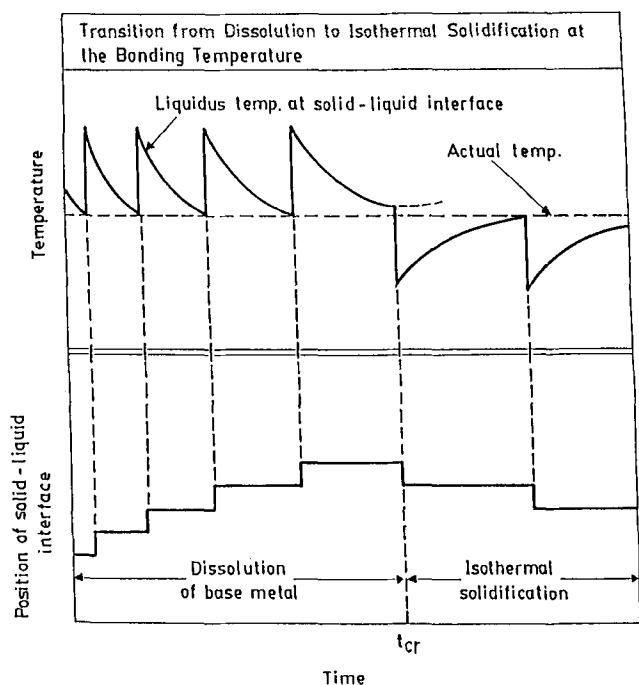
Fig. 3A—Schematic representation of the transition from dissolution to isothermal solidification.

from the actual temperature during the transitory pause and is illustrated in Figure 3A. The average temperature of all meshes in the liquid is the criterion used to assess the start of the isothermal solidification process during TLP brazing; *i.e.*, during melting, the average temperature of the liquid is generally lower than that of the brazing temperature but gradually rises because of the dilution during melting and solute diffusion into the base metal. As a result, calculations of base metal melting are continued as long as the average liquid temperature is less than the brazing temperature.

The average liquidus temperature, T_{lav}, is calculated using the equation

$$T_{lav} = T_e + Gl(C_e - C_{lav}) \qquad [14]$$

where C_{lav} is the average concentration of solute in the liquid and is given by the equation

$$C_{lav} = \Sigma \, C_i(n)/(i + 0.5) \qquad [15]$$

For the ternary alloy's situation, the equations are modified in a similar manner to Eq. [13].

F. Variable and Constant Liquid Width Situations

It is important to deduce which mesh number should draw off the liquid in order to keep the liquid width constant at the moment of advance of the solid-liquid interface. Since liquid near the solid-liquid interface is less likely to be removed due to surface tension effects, it is assumed that liquid at the center of the joint region is

expelled. For a constant liquid width situation, liquid is expelled, and it is assumed that liquid having an average composition is removed from the joint. In effect, a mesh point $i/2$ is removed just before the advance of the interface. This assumption of an average liquid composition being removed is an approximation but is a useful method of handling the problem. During modeling, $C_i(n)$ is substituted to the $(n - 1)$th mesh point just prior to the advance of the interface, where $2 < n < i$. Also, i is kept constant when the interface advances.

G. Melting of Base Metal and Solidification during the Heating Cycle from the Insert Melting Point to the Brazing Temperature

If the heating rate is very slow, it is possible for solidification to occur during the heating stage. In this case, the brazing temperature is changed to a temperature T_a during heating; *i.e.*,

$$T_a = T_e + R_h t \qquad [16]$$

where R_h is the heating time and t is the time lapse after melting of the filler metal.

REFERENCES

1. D.S. Duvall, W.A. Owczarski, and D.F. Paulonis: *Weld. J.*, 1974, vol. 53, pp. 203-14.
2. C. Nernst: *Z. Phisikal Chem.*, 1904, vol. 47, pp. 52-55.
3. J.M. Lowell and B. Chalmers: *Trans. TMS-AIME*, 1959, vol. 215, pp. 499-506.
4. Y. Nakao, K. Nishimoto, K. Shinozaki, C.H. Kang, and Y. Hori: *Q. J. Jpn. Weld. Soc.*, 1988, vol. 6, pp. 519-26.
5. I. Tuah-Poku, M. Dollar, and T.B. Massalski: *Metall. Trans. A*, 1988, vol. 19A, pp. 675-86.
6. M. Hansen: *Constitution of Binary Equilibrium Diagrams*, 2nd ed., McGraw-Hill, New York, NY, 1958.
7. R.P. Elliott: *Constitution of Binary Alloys*, 1st suppl. McGraw-Hill, New York, NY, 1965.
8. T.B. Massalski: *Binary Alloy Phase Diagrams*, ASM, Metals Park, OH, 1986.
9. H. Ikawa, Y. Nakao, and T. Isai: *Trans. Jpn. Weld. Soc.*, 1979, vol. 1, pp. 24-29.
10. Y. Nakamura and H. Esaka: *Tetsu-to-Hagané*, 1981, vol. 67 (4), p. 140.
11. A. Majdic, D. Graf, and H. Schenek: *Arch. Eisenhuettenwes.*, 1969, vol. 40, pp. 27-32.
12. P.L. Gruzin and V.V. Minal: *Fiz. Met. Metalloved.*, 1963, vol. 16, pp. 551-54.
13. H. Nakagawa, C.H. Lee, and T.H. North: University of Toronto, Toronto, Canada, unpublished research, 1989.
14. *Data Book of Metallurgy*, Jpn. Inst. Met., Sendai, Japan, 1984, Maruzen.
15. T. Matsumiya, S. Mizoguchi, Y. Veshima, and H. Esaka: *Trans. Iron Steel Inst. Jpn.*, 1984, vol. 24, pp. 873-80.